Electron impact ionization cross section of metastable $N_2(A\,\Sigma_u^+)$

P. B. Armentrout, Susan M. Tarr,[a] Ariel Dori, and Robert S. Freund

Bell Laboratories, Murray Hill, New Jersey 07974
(Received 13 May 1981; accepted 26 May 1981)

The nondissociative electron impact ionization cross section of the metastable $N_2(A\,^1\Sigma_u^+)$ state is measured from threshold to 240 eV. Rising from an appearance potential of 10.1 ± 0.6 eV, the cross section peaks at about 40 eV with a value of $(1.14 \pm 0.36) \times 10^{-16}$ cm^2. These values are extracted from the apparent ionization cross section of an N_2 beam composed of $\sim 50\%$ $N_2(A\,^1\Sigma_u^+)$ and $\sim 50\%$ $N_2(X\,^1\Sigma_g^+)$. This mixed state beam is formed by charge transfer neutralization of a 1 keV N_2^+ beam with NO. The $N_2(A\,^1\Sigma_u^+)$ cross section is normalized by measuring it relative to the ionization of a ground state N_2 beam formed by charge transfer neutralization of N_2^+ with N_2.

INTRODUCTION

Extensive studies of electron impact cross sections have been carried out both experimentally and theoretically for a number of *ground* state atoms and molecules.[1] In general, as the electron energy is increased, such cross sections rise from a threshold at the ionization potential to a peak at an electron energy roughly 4–6 times the threshold energy, before falling monotonically. Magnitudes of the peak range from 10^{-17} to over 10^{-15} cm^2 for various species. Little experimental or theoretical work has been done on electron impact ionization cross sections of *excited* species. However, knowledge of both the functional form and magnitude of such cross sections would be useful to characterize stepwise ionization processes which are believed to be important in gas discharges,[2] laser plasmas,[3] and the optogalvanic effect.[4] Experimental cross sections for excited state ionization also present a challenge to various quantum mechanical and semiclassical theories of electron impact ionization.

The only excited states for which electron impact ionization cross sections have been measured are $H(2s)$,[5] $He(2^{1,3}S)$,[6-10] $Ne(^3P_{2,0})$,[10] and $Ar(^3P_{2,0})$.[10] No reliable experimental studies concerning excited *molecular* species have been performed. Several theoretical studies of the ionization of excited atoms exist,[11-14] but examination of molecules appears limited to a calculation by Tannen[15] on $N_2(A\,^3\Sigma_u^+)$ and the work of Flannery and co-workers[12] on N_2^*, CO^*, Ne_2^*, and Ar_2^*. Other work of some relevance to this subject is that concerning photoionization of excited species.[16] Such photoionization is a serious loss mechanism for excited species in laser systems and consequently has received considerable attention.

In measurements of ionization cross sections of excited species, the major impediment has been the difficulties associated with producing sufficiently intense sources of excited states. Three techniques have been used: excitation in a discharge, excitation by electron impact, and near-resonant charge transfer neutralization of ion beams. The first method, discharge excitation, was used in early work[6,17] to study a variety of species

including metastable N_2,[17] but it suffers from being nonselective in its excitation. While the presence of excited states, electronic and vibrational, can easily be detected, extracting reliable ionization cross sections for a specific state over an extended energy range is not feasible. The second method, excitation of a thermal beam of atoms or molecules by a crossed electron beam, has been used with success to study ionization of $He(2^{1,3}S)$.[7-9] An examination[15] of N_2 excited species using this technique was largely inconclusive, determining only that an upper limit to the ionization cross section for $N_2(A\,^3\Sigma_u^+, v=3) \to N_2^+(A\,^2\Pi_u, v=1)$ at an electron energy of 25 eV is $(6 \pm 5.5) \times 10^{-16}$ cm^2.

The third technique, charge transfer neutralization, was pioneered by Peterson[18] and has been applied with good results to a variety of atomic species[19] including excited states of H,[5] He,[10] Ne,[10] and Ar.[10] The method, shown schematically in Fig. 1, involves neutralizing an ion beam in a collision cell filled with the charge transfer reactant. This reactant is chosen such that formation of a neutral in an excited state is near resonant while formation of a ground state neutral is not. The remaining unreacted ion beam is easily disposed of by electric fields. The neutral beam is now crossed by a variable energy electron beam for reionization. The ion signal which results is directly related to the electron impact ionization cross section.

In the present study, a 1 keV beam of N_2^+ is neutralized by N_2 and by NO. The ionization cross section for an N_2 beam formed by charge transfer with N_2 is found to match literature data for ionization of $N_2(X\,^1\Sigma_g^+)$. The beam formed in $N_2^+ + $ NO neutralization is found to contain $\sim 50\%$ ground state and $\sim 50\%$ excited state N_2. Reasons for identifying this excited state as $N_2(A\,^3\Sigma_u^+)$ are discussed. By measuring the ionization for this mixed state beam and subtracting the contribution from ionization of the ground state, the ionization cross section for $N_2(A^3\Sigma_u^+)$ is obtained over an extended electron energy range.

EXPERIMENTAL

Apparatus

The apparatus, shown in Fig. 2, comprises three differentially pumped chambers each having a base pressure of 2×10^{-8} Torr. The ion source, obtained

---

[a] Present address: Western Electric Engineering Research Center, Princeton, N.J. 08540.
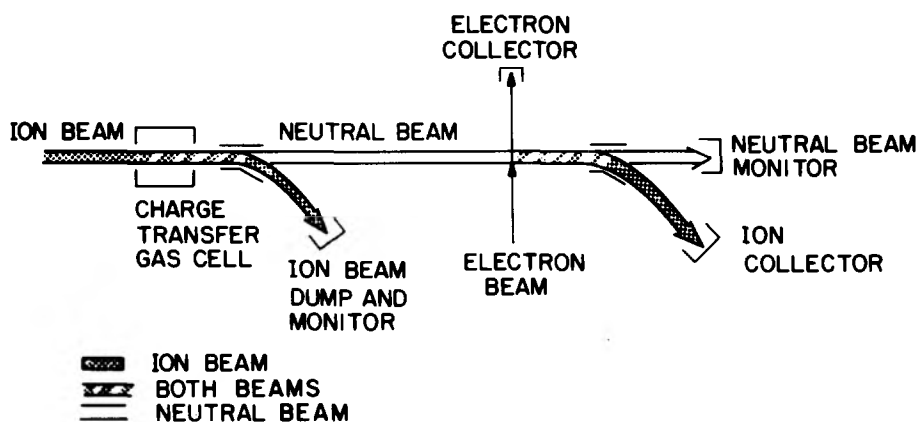
FIG. 1. Schematic representation of the charge transfer neutralization–electron impact ionization experiment.

from Colutron Research Corporation, is an electron impact sustained low voltage dc discharge[20] capable of producing an ion beam of several microamperes. Typical conditions in these experiments called for a N_2 pressure in the discharge of approximately 0.1 Torr and an anode potential of 100 V. The ions produced, which include N_2^+, N^+, N_2^{+2}, and contaminant species, are extracted and accelerated to 1 keV where they are analyzed using a Wien filter.[21] While the Wien filter, containing crossed electric and magnetic fields, is actually a velocity filter, a dispersion in m/z is obtained because all the ions nominally have the same kinetic energy. Thus, the ion beam entering the charge transfer gas cell consists of only N_2^+. A typical ion current of 150 nA is measured at the ion beam monitor in the charge transfer chamber (Fig. 2). While in operation, the background pressure in the ion source chamber is typically 1×10^{-7} Torr.

To produce a neutral beam, the gas cell located in the charge transfer chamber is filled with a gas, N_2 or

NO in these studies, to a pressure of 0.1–1.0 mTorr. The entrance and exit apertures are both $\frac{1}{8}$ in. in diameter and $\frac{1}{4}$ in. long. The cell, nominally 3 in. long, has has an effective length[22] of 8.5 ± 0.8 cm. The cell design discriminates against large angle scattering. For these experiments, this discrimination is desirable since charge transfer generally occurs at large impact parameters and small angle scattering.[23] This also means that little momentum is transferred during the charge transfer process resulting in a product neutral beam having essentially the same kinetic energy as the reactant ion beam.

The beam emerging from the charge transfer gas cell passes through a set of electric plates, the ion beam dump and monitor (Fig. 2), which deflects any unneutralized ions. An electrically isolated plate is positioned to collect these ions so that their current can be measured. Attenuation measurements, described in the Results section, are performed by measuring the transmitted ion beam at this point. The neutral beam next
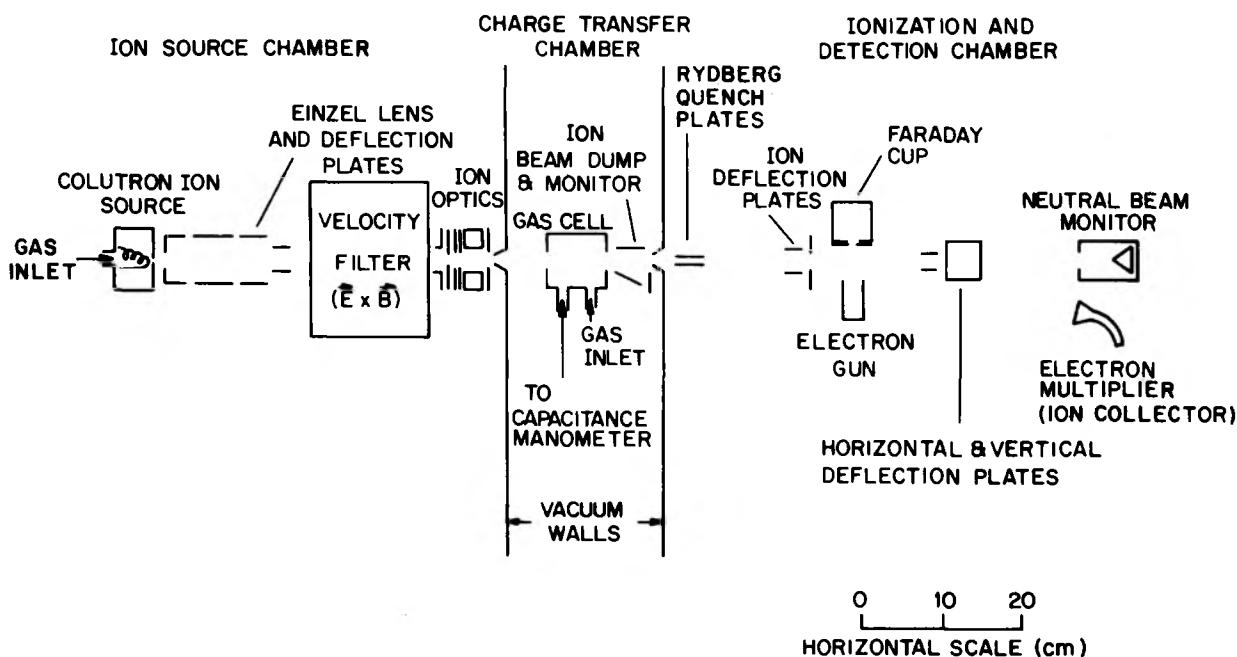

FIG. 2. Schematic diagram of the apparatus.

enters the third chamber where it passes through two additional sets of electric field plates. Their function is to further purify the beam as described in more detail in the next section.

The neutral beam now crosses the electron beam at right angles. The Pierce-type electron gun, an ARIS model ESA 1000, has been described in detail previously.[24] The electron beam has an energy spread of ~0.3 eV (FWHM) and provides a constant current of ~40 μA for electron energies above about 10 eV. The ability of this system to correctly measure relative ionization cross sections was carefully checked using He, Ar, Xe, and N₂. It was found that for a particular set of electron gun focusing conditions, results for electron energies below about 30 eV agreed with literature data.[25,26] Above 30 eV, systematic deviations for all systems were observed under all electron gun conditions. These deviations are attributable to an energy dependent focusing of the electron beam. As this focus changes, the fraction of measured electrons which actually interacts with the neutral beam changes and, as a consequence, the apparent relative ionization cross section also changes. Thus, above 30 eV the ionization cross section is determined by making a measurement relative to a known system. This procedure is discussed in more detail in a later section.

While the electron energy scale could be calibrated by measuring the potential at which the electron current vanishes,[25] another means, giving comparable results, was chosen as being more reliable. A phototube was mounted perpendicularly to the electron and neutral beams. Using an interference filter centered at 3371 Å (100 Å bandwidth), the optical emission from the second positive system of molecular nitrogen, primarily N₂ $(C\,^3\Pi, v'=0)-N_2(B\,^3\Pi, v''=0)$, was monitored. To obtain sufficient intensity, additional N₂ was allowed into the electron beam–neutral beam interaction region to a pressure of about 10^{-6} Torr. The emission as a function of electron energy was compared with a literature excitation function[27] to obtain the contact potential and space charge depression of the potential in the center of the electron beam. The value obtained, 1.8 ± 0.1 eV was checked periodically.

The ions formed by electron impact are deflected by a final pair of plates into a Channeltron electron multiplier operated in a pulse counting mode. The multiplier is shielded by a box biased at +2 V to prevent random thermal energy ions from contributing to the ion signal. The multiplier is also shielded from seeing the electron beam–neutral beam interaction region so that high energy photons created in this region do not contribute. The output pulses enter an amplifier–discriminator and then a PDP-8/L computer operated as a multichannel scaler. The computer also collects a digitized signal for the electron beam current.

It is important to note that the final deflecting plates separate ions of different mass. This is because N⁺ ions produced in dissociative ionization have nominally the same laboratory velocity as the precursor N₂ molecules and thus half the energy. Thus, these atomic ions will be deflected through twice the angle as the N₂⁺

ions and so miss the detector. Similarly, multicharged ions produced at higher electron energies are deflected through larger angels than singly charged ions. The result is that nondissociative single ionization rather than total ionization is measured.

The neutral beam is monitored by a modified Faraday cup using secondary electron emission. The beam hits a conical CuBe surface mounted inside a Faraday cup. Electrons emitted from this surface are then collected by the grounded Faraday cup. The CuBe cone is biased at –20 V to increase the efficiency at which emitted electrons are collected. The neutral beam current is related to the secondary electron current by γ, the secondary electron emission coefficient. The value of γ is discussed below.

Background ions

Dixon, Harrison, and Smith[10] give an extensive discussion of the kinds of background inherent in measurements of the kind conducted in this study. Only those sources of noise which plagued the present experiments will be discussed here. Other sources are believed to be negligible.

By far the most intense background in these experiments is ions produced by charge stripping collisions of the fast neutral beam[28] with background gas. Even with a background pressure during operation of only 4×10^{-8} Torr in the third chamber, the contribution to the measured ion signal is appreciable and can easily exceed the signal due to electron impact ionization. The ion deflection plates placed just before the electron gun (Fig. 2) remove as many of these stripped ions as possible but cannot eliminate those formed further along the neutral beam path.

Fortunately, this spurious signal can be distinguished by two techniques. If the electron beam is modulated, the desired signal is also modulated while the stripped ion signal remains dc. Alternatively, a dc electron beam is swept in energy from below the ionization potential of the neutral beam. This low energy portion of the sweep establishes the level of the background. Both methods give comparable results. The latter technique was used for the data reported in this study.

Another source of background in these experiments is due to electron impact ionization of nitrogen molecules in long-lived high-Rydberg states. The Rydberg quench plates (Fig. 2), designed to field ionize these excited molecules, have a 0.25 in. gap and a 6 kV potential across them. The resultant field of approximately 10^4 V/cm should ionize all Rydbergs with $n\ge16$.[29] Many of the Rydbergs with low n decay radiatively during the 4 μs flight time between the gas cell and the electron gun. Using lifetime estimates based on hydrogenic orbitals,[30,31] all species with $n\le9$ decay. The angular momentum state l of the Rydbergs determines the lifetime of species with $10\le n\le15$.[30,31] It has been estimated that for H₂⁺ + H₂ charge transfer, only 9% ± 3% of the Rydbergs formed have $l\ge3$.[32] If this is also the case in the present studies, 90% of the remaining Rydbergs are also expected to radiatively decay. It should also be noted that the decay of molecular Rydbergs can

involve predissociation and vibrational autoionization[33] in addition to radiative and electronic autoionization, whereas atomic Rydbergs can decay only by the latter two mechanisms. These considerations explain why background due to Rydbergs is apparently negligible in the present work while in previous studies[4,10,19] using the charge transfer technique to study atomic beams, such background was appreciable.

A final source of background, at first attributed to Rydberg ionization, appears to result from electrons scattering from the interaction region and being accelerated by potentials on deflection plates and the wires which supply these potentials. These electrons produce ions by a variety of means such as ionization of background gas and secondary ion emission from impacted surfaces. Electron leakage is particularly severe at the lowest electron energies where the electron beam is most poorly focused. The problem was resolved by shielding many of the wires, shielding the ion collector, and by using primarily negative potentials on the deflecting plates.

RESULTS

Charge transfer cross sections and ion beam composition

Attenuation experiments were performed to characterize the reactant ion beam and measure charge transfer cross sections. Such experiments may be under-
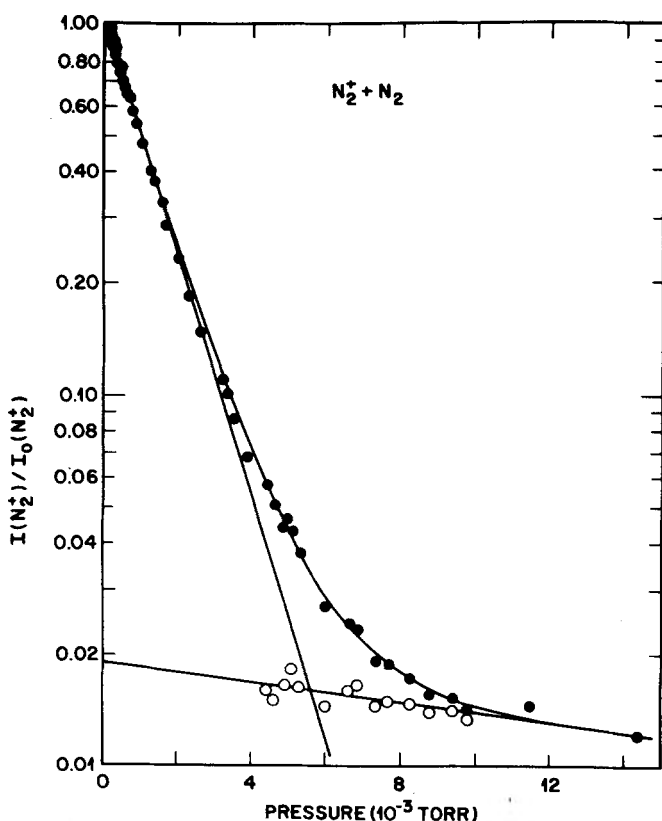

FIG. 3. Attenuation of a 1 keV N_2^+ beam by N_2 as a function of the pressure of the attenuating gas. The line drawn through the data (●) is the sum of the two straight lines shown. The circles are the contribution remaining after the line determined at low pressures by a least squares fit is subtracted from the data.
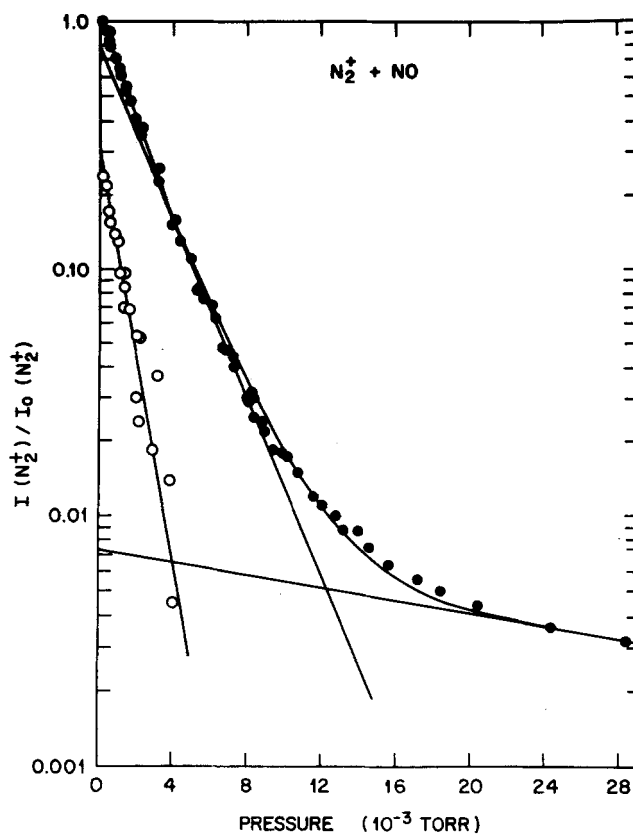

FIG. 4. Attenuation of a 1 keV N_2^+ beam by NO as a function of the pressure of the attenuating gas. The line drawn through the data is the sum of the three straight lines shown. The circles are the contribution remaining after subtracting the two lines determined by a least squares fit to the high pressure data.

stood by examining the following formula for the transmission of ions through a cell filled with gas:

$$I/I_0 = \exp(-n\sigma d) \quad , \tag{1}$$

where I is the transmitted ion current, I_0 is the ion current at zero pressure, n is the number density of the gas (α pressure P), σ is the interaction cross section, and d is the interaction length. A plot of $\ln(I/I_0)$ vs P has a slope directly proportional to the cross section. If the ion beam contains a fraction g of excited ions with an interaction cross section σ*, then the fraction of transmitted current is given by

$$I/I_0 = (1-g)\exp(-n\sigma d) + g\exp(-n\sigma^* d) \quad . \tag{2}$$

Again by plotting $\ln(I/I_0)$ vs P, the values for g, σ, and σ* may be obtained.[34,35] Strictly speaking, the cross sections derived below are upper limits to the charge transfer cross sections since other processes such as elastic scattering may also attenuate the beam. However, at 1 keV beam energy, the charge transfer component of the total interaction cross section is probably the dominant contribution.

The results of attenuation measurements for a 1 keV N_2^+ beam in N_2 and NO are shown in Figs. 3 and 4, respectively. Attenuation in N_2 shows an apparent two component system. The cross section for the major component is $(28 \pm 2) \times 10^{-16}$ cm^2. This is in excellent

agreement with literature data[36-41] for the charge transfer cross sections of $N_2^+ + N_2$ and thus lends credence to the assumption made in the previous paragraph. The minor component has a very small cross section of $(1.2 \pm 1.0) \times 10^{-16}$ cm^2. We believe this minor component is actually due to sequential elastic collisions which deflect N_2^+ ions back into the beam. The fact that the same effect is observed in the NO system (Fig. 4) is consistent with this interpretation. Thus, N_2^+ attenuation in N_2 shows no excited state contribution. Smith,[41] in a careful examination of $N_2^+ + N_2$ charge transfer, also found no structure attributable to excited species. While this could mean either that $g = 0$ or that $\sigma = \sigma^*$, the latter explanation seems more likely and is consistent with the value of g derived below.

Attenuation of N_2^+ in NO (Fig. 4) clearly shows a two component system (neglecting the curvature at high pressures due to secondary collisions). By extrapolating the high pressure data back to zero pressure, we find $(1-g) = 0.75$. This component, assumed to be N_2^+ $(X\,^2\Sigma_g^+)$, has a cross section of $(15 \pm 2) \times 10^{-16}$ cm^2. The cross section for the second component, assumed to be $N_2^+(A\,^2\Pi_u)$, is obtained by subtracting the contribution of the first component from the raw data. This yields the open circles shown in Fig. 4. The cross section is $(35 \pm 4) \times 10^{-16}$ cm^2. Only one previous measurement of the charge transfer cross section for N_2^+ in NO has been made.[40] A value of about 7×10^{-16} cm^2 was obtained, in fair agreement with our result; however, the measurement was made relative to another reaction, and as such, was stated to be uncertain.

The fraction of excited ions measured (0.25) is in reasonable accord with a calculation which predicts 0.37 in the $A\,^2\Pi_u$ state and negligible amounts of other excited species. The calculation assumes the ions are formed by 60 eV electron impact and radiatively decay during the 6 μs ion flight time. We use ionization probabilities and state lifetimes reported by Maier.[42] The experimental value is lower than that calculated because the higher pressures of our source lead to collisional quenching of excited species.

Attenuation measurements provide no information regarding the vibrational population of the N_2^+ beam. The calculation performed above predicts most molecules in the X state are in $v = 0$ with some (~ 0.4) in the $v = 1, 2$ states. A substantial fraction of ions in the A state are predicted to be vibrationally excited. The high pressure nature of the ion source undoubtedly affects these populations,[43] probably much more than the electronic state distribution.

Relative ionization cross sections: Threshold region

Beams of N_2 neutrals, designated $N_2(N_2)$ and $N_2(NO)$, were obtained by neutralizing the N_2^+ ion beam with N_2 and with NO, respectively. The ion signals obtained by electron impact ionization of these two neutral beams, $I^+(N_2)$ and $I^+(NO)$ are shown in Fig. 5. The $I^+(N_2)$ spectrum shown is quite typical and was accumulated in 5 h. The dc background level is about 2.5 times the signal shown at 25 eV. The $I^+(NO)$ spectrum shown took 30 h to accumulate and is the sum of several separate runs.
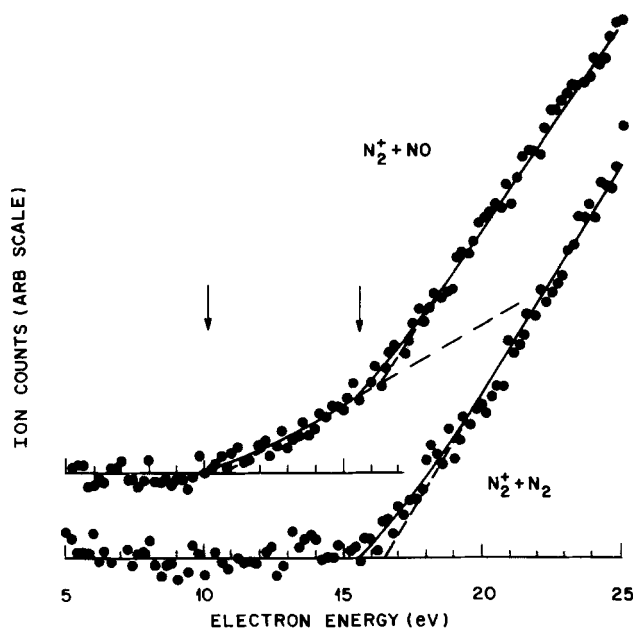

FIG. 5. The ion signal as a function of electron energy (corrected for space charge and contact potentials) resulting from electron impact ionization of an N_2 beam produced by neutralization of N_2^+ with N_2 (lower points) and with NO (upper points). The solid curve drawn through the lower points is the data of Ref. 25 normalized at 25 eV. Straight lines drawn through the upper points are determined by linear regression analysis. The arrows indicate the ionization potential of N_2 $(X\,^1\Sigma_g^+)$, 15.58 eV, and the appearance potential of the upper points, 10.1 ± 0.4 eV, determined as discussed in the text.

The background level, about 6.5 times the signal shown at 25 eV, is larger in this case because higher NO pressures which are needed to obtain a comparable neutral beam flux lead to more stripping. The baseline levels shown are determined by averaging all points (some of which are not shown in Fig. 5) at energies below the apparent ionization potentials.

The solid line through $I^+(N_2)$ (Fig. 5) is the cross section of Rapp and Englander-Golden[25] normalized to our data at 25 eV. The curvature is due to ionization of $N_2(X\,^1\Sigma_g^+)$ to the three N_2^+ states $X\,^2\Sigma_g^+$, $A\,^2\Pi_u$, and $B\,^2\Sigma_u^+$ at 15.58, 16.70, and 18.75 eV, respectively.[44,45] The good agreement demonstrates that the $N_2(N_2)$ beam is exclusively $N_2(X\,^1\Sigma_g^+)$. There is the possibility that some vibrational excitation is present; indeed, calculations[46] suggest approximately 4% of the N_2 should be in $v = 1$. The data do not preclude this possibility but indicate that most of the N_2 is in the $v = 0$ level.

Ionization of $N_2(NO)$ is substantially different from that of $N(N_2)$. Two linear regions intercepting one another at 16.5 ± 0.6 eV are evident. This is approximately the same energy as the apparent threshold for $N_2(N_2)$ ionization found by linear extrapolation to the baseline (16.3 eV). This indicates that a substantial portion of the $N_2(NO)$ beam is in the $N_2(X)$ state. The remaining contribution to the $N_2(NO)$ ionization accounts for the linear portion at lower energies. From a linear extrapolation to the baseline, the appearance potential for $I^+(NO)$ is found to be 10.8 ± 0.6 eV, where the error

is one standard deviation of 16 individual measurements. Assuming the same curvature as is observed for the $N_2(X)$ state, the corrected ionization potential is 10.1 ±0.6 eV.

Normalized ionization cross section for the mixed state beam

As discussed in the experimental section, the data above 30 eV must be corrected for electron beam focusing effects. In the present study, this was achieved by comparing the signal from ionization of the $N_2(N_2)$ beam with literature data. Because we measure only nondissociative ionization, Rapp and Englander-Golden's total ionization cross sections[25] are modified by their measurements of the dissociative ionization cross sections[26,47] and further modified by Märk's[48] values for ionization to N_2^{2+}. This derived curve, listed in Table I, is in reasonable agreement with a measurement of Märk.[48,49] Using this literature cross section, the data for ionization of the $N_2(NO)$ beam was corrected. The result, $\sigma[N_2(NO)]$ is compiled in Table I and shown graphically in Fig. 6.

In principal, the relative ionization cross sections may be placed on an absolute scale[51] using

$$\sigma = I^* A^0 v^0 / w F^0 F^- \quad , \qquad (3)$$

TABLE I. Nondissociative electron impact ionization cross sections.

E(eV)	$\sigma(N_2, X\,^1\Sigma_g^+)^{a,b}$	$\sigma[N_2(NO)]^{a,d}$	$\sigma(N_2, A\,^3\Sigma_u^+)^{a,d}$
11		0.02	0.04
12		0.038	0.076
13		0.071	0.142
14		0.104	0.208
15		0.138	0.276
16	0.021	0.181	0.341
18	0.129	0.301	0.473
20	0.270	0.44	0.61
22	0.418	0.59	0.76
24	0.565	0.73	0.90
26	0.714	0.86	1.01
28	0.865	0.96	1.06
30	1.01	1.05	1.09
32	1.12	1.12	1.12
36	1.31	1.22	1.13^c
40	1.46	1.29	1.12^c
45	1.60	1.38	1.16^c
50	1.69	1.41	1.13^c
55	1.75	1.44	1.13
60	1.81	1.43	1.05
70	1.86	1.46	1.06
80	1.90	1.45	1.00
100	1.90	1.43	0.96
120	1.87	1.38	0.89
160	1.78	1.29	0.80
200	1.69	1.22	0.75
240	1.58	1.14	0.70

^{a}In units of 10^{-16} cm^2.
^{b}Derived from data of Rapp and Englander-Golden[25] and Rapp et al.[26] See the text.
^{c}Because of scatter in the data, we estimate the peak in the cross section to be at 40 eV and to have a value of 1.14×10^{-16} cm^2.
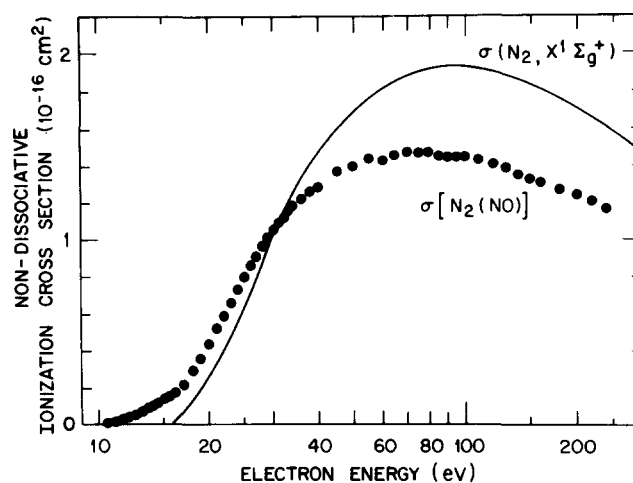^{d}This study. See the text.

FIG. 6. The nondissociative electron impact ionization cross section as a function of electron energy for $N_2(X\,^1\Sigma_g^+)$ (full line) derived from literature data (see the text) and for N_2 produced by charge transfer neutralization of N_2^+ with NO (points).

where σ is the ionization cross section, I^* is the ion signal, A^0 and v^0 are the area and velocity of the neutral beam, w is the width of the neutral beam along the electron beam, and F^0 and F^- are the neutral beam and electron beam fluxes. However, as discussed above, there is uncertainty in F^-, the electron beam flux actually interacting with the neutral beam. Thus, the absolute scale is determined using a relative technique described below.

Ionization measurements are made on $N_2(N_2)$ and $N_2(NO)$ beams holding electron gun conditions constant. Neutral beam conditions are kept as similar as possible within the constraints of the different charge transfer cross sections. Thus, the quantities A^0, v^0, w, and F^- are constants for a given electron energy E. From Eq. (3), this means that

$$\frac{\sigma(E, NO)}{\sigma(E, N_2)} = \frac{I^*(E, NO)/F^0(NO)}{I^*(E, N_2)/F^0(N_2)} \quad , \qquad (4)$$

where the NO and N_2 in parentheses are shorthand notation for a measurement on $N_2(NO)$ and $N_2(N_2)$ beams. As noted above, the neutral beam flux is monitored using secondary electron emission such that we directly measure γF^0 rather than F^0. This modifies Eq. (4) to yield

$$\frac{\sigma(E, NO)/\gamma(NO)}{\sigma(E, N_2)/\gamma(N_2)} = \frac{I^*(E, NO)/\gamma(NO)F^0(NO)}{I^*(E, N_2)/\gamma(N_2)F^0(N_2)} \quad . \qquad (5)$$

The quantity on the right-hand side is found by measuring I^* and γF^0 while varying the charge transfer gas pressure. The result, for both N_2 and NO, is that I^* is linear with γF^0, as expected. To find $\sigma(E, NO)/\sigma(E, N_2)$, a final key assumption is made, namely, $\gamma(NO) \cong \gamma(N_2)$. Utterback and Van Zyl[52] have shown this to be true for 100–200 eV N_2 beams impacting on gold surfaces. It is most certainly also true for a 1 keV N_2 beam impacting a CuBe surface.[53]

The value for the right-hand side of Eq. (5) at 28.2 eV is 1.10 ± 0.30. This value is used to place the relative ionization cross section for the $N_2(NO)$ beam on the same absolute scale as the results for the $N_2(N_2)$ beam,
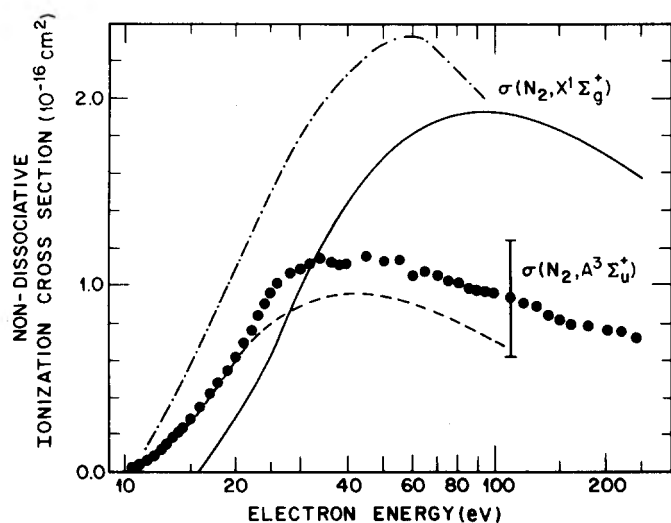
FIG. 7. The nondissociative electron impact ionization cross section for $N_2(X^1\Sigma_g^+)$ (full line) and $N_2(A^3\Sigma_u^+)$ (points). The other lines are calculations of $N_2(A^3\Sigma_u^+) \to N_2^+(A^2\Pi_u)$ ionization by Ton-That and Flannery[12] (dot–dashed line) and Tannen[15] (dashed line).

assumed identical to the Rapp and Englander-Golden cross section. The final result is shown in Fig. 6. Values for the right-hand side of Eq. (5) were also obtained at several other electron energies and agreed well with the curve exhibited.

Normalized ionization cross section of excited N₂

As noted above, a substantial fraction of the $\sigma(NO)$ cross section appears to be due to ground state ionization. If the fraction of excited species in the $N_2(NO)$ beam is given by f, then it should be true that

$$\sigma[N_2(NO)] \equiv \sigma(NO) = (1 - f)\sigma_x + f\sigma_A \quad , \tag{6}$$

where σ_x is the ionization cross section for $N_2(X^1\Sigma_g^+)$ given in Table I and σ_A is the ionization cross section for excited N_2, shown below to be the $N_2(A^3\Sigma_u^+)$ state. Since $\sigma(NO)$ and σ_x are now known, a knowledge of f will allow σ_A to be extracted.

To obtain f, we assume that σ_A is linear from near threshold to about 20 eV. The signal in excess of that predicted by a linear extrapolation of the low energy portion of $\sigma(NO)$ (Fig. 5) is $(1 - f)\sigma_x$. Comparing this value with σ_x using the absolute signal established above yields f directly, 0.50 ± 0.16. Because of the uncertainties in calibrating the absolute cross section scale, estimated to be 28%, and in fitting a line through the low energy region of $\sigma(NO)$ (16%) the error in f is large. Using this value of f, the ionization cross section for N_2 excited species, shown in Fig. 7, and listed in Table I, is derived. The absolute error in this curve is ±32%. The error in the relative shape is estimated to be ±10%.

In related experiments, Utterback and Van Zyl[52] determined f for a $N_2(NO)$ beam at lower kinetic energies (200 eV or less). Their experimental conditions (source, beam energy, and charge transfer conditions) are sufficiently removed from those in the present study

that no quantitative comparison can be made. However, the fact that their values for f (0.03–0.09) are substantially lower than ours suggests that f is quite dependent on experimental conditions.

DISCUSSION

Identity of excited state: Predictions

Two factors are expected to dominate the state distribution of the products of a charge transfer reaction. The first, energy resonance, is expected to be most important at low collision energies where translational energy is not available to overcome energy defects. The second, Franck–Condon (F–C) overlap, is expected to be the major effect in the sudden limit at high collision energies. At 1 keV collision energy, it is expected that both factors will be influential. Similar considerations have been previously discussed for lower collision energies.[52]

It is somewhat surprising that ionization of the $N_2(N_2)$ beam shows little evidence for vibrational excitation since at a collision energy of 1 keV, 500 eV is available for transfer. That little if any excitation is observed is a dramatic demonstration of the role of energy resonance and F–C factors in charge transfer reactions. Certainly, the process

$$\overline{N}_2^+(X, v) + N_2(X, v = 0) \to \overline{N}_2(X, v = 0) + N_2^+(X, v) \quad , \tag{7}$$
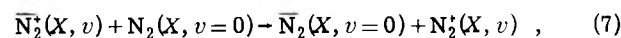
where the bar indicates the fast molecule, is favored by resonance considerations. Even considering electronically excited N_2^+, the resonant process

$$\overline{N}_2^+(A, v) + N_2(X, v = 0) \to \overline{N}_2(X, v = 0) + N_2^+(A, v) \tag{8}$$
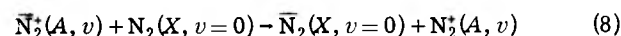
still yields N_2 in its ground vibrational and electronic state. As noted in the Results section, calculations which include the F–C factors predict only 4% of the product N_2 should be in the $v = 1$ level.

The role of energy resonance is also undoubtedly important in the charge transfer neutralization of N_2^+ by NO. Indeed, such considerations led Utterback and Van Zyl[52] to conclude that the metastable N_2 formed by such charge transfer was $N_2(A^3\Sigma_u^+)$, although their experiment had no way of verifying this. The relevant energy level diagram is shown in Fig. 8. Also included in this diagram are approximate Franck–Condon factors for the various transitions. What is immediately obvious from Fig. 8 is that good energy resonances exist for production of both the X and A states of N_2. The $N_2(B^3\Pi_g)$ state is at least 1.03 eV out of resonance. Consideration of F–C factors indicates formation of $N_2(X)$ is favored over $N_2(A)$, but that $NO^+(X)$ is more favorable than $NO^+(a)$. Consideration of vibrationally excited $N_2^+(X)$ reactant only serves to increase the F–C overlaps for production of both $N_2(X)$ and $N_2(A)$.

The $N_2^+(A^2\Pi_u)$ reactant state also needs to be considered. Since its charge transfer cross section is larger than that for the $N_2(X)$ state, this excited ion is responsible for approximately 40% of the N_2 neutrals formed at the pressures of NO used in these studies. Examination of a diagram analogous to Fig. 8 shows formation of $N_2(A) + NO^+(X)$ is still resonant but now favors higher

vibrational levels. The same is true for $N_2(X) + NO^*(a)$ production. In addition, a good resonance exists for $N_2(X) + NO^*(b\,^3\Pi)$ formation (energy defect is 0.14 eV). The possibility of $N_2(B\,^3\Pi_g) + NO^*(X)$ products also now exists since this process is only off resonance by 0.09 eV. It should be noted, however, that even if the $N_2(B)$ state formed, over half would radiatively decay to $N_2(A)$ during the flight time between the gas cell and the electron gun.

Our general conclusion based on the energy level diagram is that the excited state of the $N_2(NO)$ beam should be predominantly $N_2(A\,^3\Sigma_u^+)$. It is difficult to predict whether $N_2^+(X)$ or $N_2^+(A)$ is the primary precursor ion; however, the results of Utterback and Van Zyl[52] suggest $N_2^+(A)$ may be the more important. While it is not feasible to suggest specific vibrational populations for either the $N_2(X)$ or $N_2(A)$ states formed, it seems likely that the A state is vibrationally excited.

Identity of excited state: Experiment

A direct check on the identity of the excited species is provided by the appearance potential for ionization of the $N_2(NO)$ beam. Thresholds for ionization of $N_2(A^3\Sigma_u^+)$ to the X, A, or B states of N_2^+ are expected to occur at 9.35, 10.47, and 12.52 eV, respectively. Examination of the molecular orbital configurations of the appropriate N_2 and N_2^+ states (Table II) shows that the first ionization process $N_2(A) \rightarrow N_2^+(X)$, requires a two electron transition, relaxation of one electron and loss of another. Such a two electron process is generally considered to be unlikely. Indeed, calculations[12,15] consider only $N_2(A) \rightarrow N_2^+(A)$ ionization, a one electron process. If the $N_2(B)$ state is present in the $N_2(NO)$ beam, its ioniz-
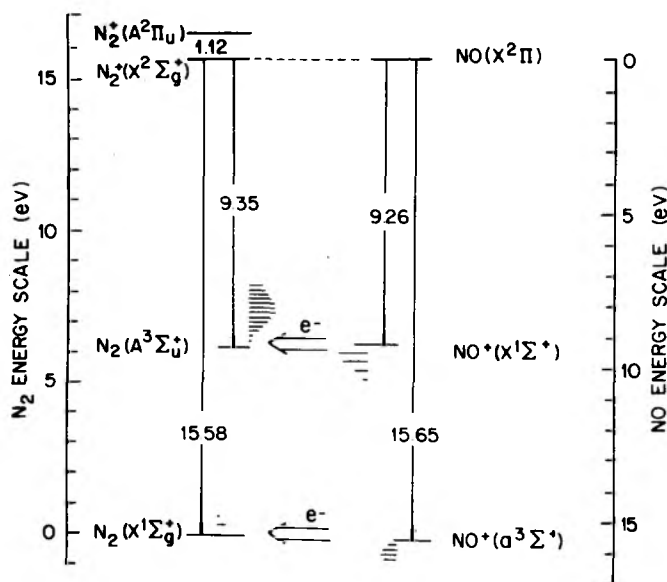

FIG. 8. Energy level diagram showing the states of N_2, N_2^+, NO, and NO$^+$ involved in charge transfer of N_2^+ with NO. The NO energy scale is inverted with its zero placed at the level for $N_2^+(X\,^2\Sigma_g^+$, $v = 0$). Energies shown are for transitions between the ground rotational and vibrational levels of the appropriate states. Approximate Franck–Condon factors are indicated by the lengths of lines for the product vibrational states.

TABLE II. Molecular orbital configuration of N_2 and N_2^+ states.

| Species | State | Molecular orbital configuration | | | |
		$(1\pi_u)$	$(3\sigma_g)$	$(1\pi_g)$	Other
N_2^+	$B\,^2\Sigma_u^+$	4	2	0	$-2\sigma_u$
		3	1	1	
	$A\,^2\Pi_u$	3	2	0	
	$X\,^2\Sigma_g^+$	4	1	0	
N_2	$B\,^3\Pi_g$	4	1	1	
	$A\,^3\Sigma_u^+$	3	2	1	
	$X\,^1\Sigma_g^+$	4	2	0	

ation to $N_2^+(X)$, a one electron transition, would be expected at 8.23 eV.

The measured appearance potential of the $N_2(NO)$ beam is 10.1 ± 0.6 eV. This is definitely higher than either of the values for $N_2(A)$ or $N_2(B) \rightarrow N_2^+(X)$ ionization. It is within experimental error of the $N_2(A) \rightarrow N_2^+(A)$ ionization threshold of 10.47 eV. Considering our expectation that the $N_2(A)$ molecules in our beam are vibrationally excited, the 10.1 ± 0.6 eV potential is in excellent agreement. The difference corresponds to 2 ± 4 quanta of vibrational excitation.

Ionization cross section of $N_2(A\,^3\Sigma_g^+)$

The nondissociative electron impact ionization cross section of the now identified $N_2(A\,^3\Sigma_u^+)$ state is shown in Fig. 7. The shape of the curve is quite reasonable as it peaks near four times the appearance potential and then drops off slowly. It is, at first, surprising that the peak value of $(1.14 \pm 0.36) \times 10^{-16}$ cm^2 is less than the value for ionization of ground state N_2 1.90×10^{-16} cm^2. However, since the $1\pi_g$ orbital ionized in the A state and the $3\sigma_g$ orbital ionized in the X state are both linear combinations of $2p$ atomic orbitals, they should have comparable sizes. In addition, the A state $1\pi_g$ orbital is occupied by only one electron while the X state $3\sigma_g$ orbital is occupied by two. These simple considerations predict $\sigma(N_2, A)$ to be about one half $\sigma(N_2, X)$ but neglect ionization to higher states of N_2^+ as well as more subtle effects.

Two theoretical calculations of $N_2(A\,^3\Sigma_u^+) \rightarrow N_2^+(A\,^2\Pi_u)$ ionization are shown in Fig. 7. The upper curve is by Ton-That and Flannery[12] who used a binary-encounter method. The lower curve is from Tannen[15] who used the Gryzinski semiclassical theory. Such calculations have proven to be in reasonable agreement with experimental results for ionization of the rare gas metastables[11,12] and ground state N_2.[54] For the present results, the calculations are also in fair agreement with experiment. It must be recalled, however, that the experimental cross section undoubtedly includes ionization of $N_2(A\,^3\Sigma_u^+)$ to states in addition to $N_2^+(A\,^2\Pi_u)$.

ACKNOWLEDGMENT

[1]L. J. Kieffer and G. H. Dunn, Rev. Mod. Phys. **38**, 1 (1966); M. R. H. Rudge, *ibid.* **40**, 564 (1968); H. S. W. Massey and E. H. S. Burhop, *Electronic and Ionic Impact Phenomena* (Oxford University, London, 1969), Vol. I.

[2]W. F. Bailey, W. H. Long, P. Bletzinger, and A. Garscadden, 25th Annual Gaseous Electronics Conference (London, Ontario, Canada, October 1972).

[3]L. Vriens, J. Appl. Phys. **49**, 3814 (1978); J. B. Laudenslager, *Kinetics of Ion–Molecule Reactions*, edited by P. Ausloos (Plenum, New York, 1979), p. 405.

[4]K. C. Smyth and P. K. Schenk, Chem. Phys. Lett. **55**, 466 (1978).

[5]A. J. Dixon, A. von Engel, and M. F. A. Harrison, Proc. R. Soc. London Ser. A **343**, 333 (1975); P. Defrance, W. Claeys, A. Cornet, and G. Poulaert, J. Phys. B **14**, 111 (1981).

[6]W. L. Fite and R. T. Brackman, Proceedings of the 6th International Conference on Ionization Phenomena in Gases, Paris, 1963, p. 21.

[7]L. Vriens, T. F. M. Bonsen, and J. A. Smit, Physica (Utrecht) **40**, 229 (1968).

[8]D. R. Long and R. Geballe, Phys. Rev. A **1**, 260 (1970).

[9]W. Shearer-Izumi and R. Botter, J. Phys. B **7**, 125 (1974).

[10]A. J. Dixon, M. F. A. Harrison, and A. C. H. Smith, J. Phys. B **9**, 2617 (1976); A. J. Dixon, M. F. A. Harrison, and A. C. H. Smith, Abstracts of the *Eighth International Conference on the Physics of Electronic and Atomic Collisions* (Institute of Physics, Beograd, Yugoslavia, 1973), Vol. 1.

[11]L. Vriens, Phys. Lett. **8**, 260 (1964); L. Vriens and A. H. M. Smeets, Phys. Rev. A **22**, 940 (1980).

[12]D. Ton-That, S. T. Manson, and M. R. Flannery, J. Phys. B **10**, 621 (1977); D. Ton-That and M. R. Flannery, Phys. Rev. A **15**, 517 (1977); K. J. McCann and M. R. Flannery, Appl. Phys. Lett. **34**, 543 (1979).

[13]I. R. Taylor, A. E. Kingston, and K. L. Bell, J. Phys. B **12**, 3093 (1979).

[14]J. A. Kunc, J. Phys. B **13**, 587 (1980); G. Peach, J. Phys. B **1**, 1088 (1968); *ibid.* **3**, 328 (1970); *ibid.* **4**, 1670 (1971).

[15]P. D. Tannen, thesis (Air Force Institute of Technology, 1973) (University Microfilms, Ann Arbor, Mich., order No. 74-14940).

[16]A. Msezane and S. T. Manson, Phys. Rev. Lett. **35**, 364 (1975); K. J. McCann and M. R. Flannery, Appl. Phys. Lett. **31**, 599 (1977); C. Duzy and H. A. Hyman, Phys. Rev. A **22**, 1878 (1980); A. V. Smith, J. E. M. Goldsmith, D. E. Nitz, and S. J. Smith, *ibid.* **22**, 577 (1980); M. S. Pindzola, *ibid.* **23**, 201 (1981); A. L. Roche, K. Kirby, S. L. Guberman, and A. Dalgarno, J. Electron Spectrosc. Relat. Phenom. (to be published).

[17]S. N. Foner and R. L. Hudson, J. Chem. Phys. **37**, 1662 (1962); **45**, 40 (1966).

[18]J. R. Peterson, *Atomic Collision Processes*, edited by M. R. C. McDowell (North-Holland, Amsterdam, 1964), p. 465.

[19]E. Brook, M. F. A. Harrison, and A. C. H. Smith, J. Phys. B **11**, 3115 (1978).

[20]M. Menzinger and L. Wahlin, Rev. Sci. Instrum. **40**, 102 (1969).

[21]L. Wahlin, Nucl. Instrum. Methods **27**, 55 (1964).

[22]E. W. Rothe, L. L. Marino, R. H. Neynaber, P. K. Rol, and S. M. Trujillo, Phys. Rev. **126**, 598 (1962).

[23]K. J. McCann, M. R. Flannery, J. V. Hornstein, and T. F. Moran, J. Chem. Phys. **63**, 4998 (1975).

[24]K. C. Smyth, J. A. Schiavone, and R. S. Freund, J. Chem. Phys. **59**, 5225 (1973).

[25]D. Rapp and P. Englander–Golden, J. Chem. Phys. **43**, 1464 (1965).

[26]D. Rapp, P. Englander–Golden, and D. D. Briglia, J. Chem. Phys. **42**, 4081 (1965).

[27]E. Kisker, Z. Phys. **257**, 51 (1972).

[28]N. G. Utterback and G. H. Miller, Phys. Rev. **124**, 1477 (1961); N. G. Utterback, *ibid.* **129**, 219 (1963).

[29]J. A. Schiavone, D. E. Donohue, D. R. Herrick, and R. S. Freund, Phys. Rev. A **16**, 48 (1977).

[30]H. A. Bethe and E. E. Salpeter, *Quantum Mechanics of One and Two Electron Atoms* (Springer, Berlin, 1957).

[31]N. V. Fedorenko, V. A. Ankudinov, and R. N. Illin, Sov. Phys. Tech. Phys. **10**, 461 (1965).

[32]Y. B. Band, J. Phys. B **7**, 2072 (1974).

[33]S. M. Tarr, J. A. Schiavone, and R. S. Freund, J. Chem. Phys. **74**, 2869 (1981).

[34]B. R. Turner, J. A. Rutherford, and D. M. J. Compton, J. Chem. Phys. **48**, 1602 (1968); R. F. Mathis, B. R. Turner, and J. A. Rutherford, *ibid.* **49**, 2051 (1968).

[35]M. Vujovic, M. Matic, B. Cobic, and Y. S. Gordeev, J. Phys. B **5**, 2085 (1972); M. Vujovic, M. Matic, B. Cobic, and P. Hvelplund, *ibid.* **10**, 3699 (1977).

[36]H. W. Berry, Phys. Rev. **74**, 848 (1948).

[37]S. N. Ghosh and W. F. Sheridan, J. Chem. Phys. **27**, 1436 (1957).

[38]N. G. Utterback and G. H. Miller, Rev. Sci. Instrum. **32**, 1101 (1961).

[39]E. Gustafsson and E. Lindholm, Ark. Fys. **18**, 219 (1961).

[40]R. F. Stebbings, B. R. Turner, and A. C. H. Smith, J. Chem. Phys. **38**, 2277 (1963).

[41]A. Smith, thesis (Virginia Polytechnic Institute, 1977) (University Microfilms, Ann Arbor, Mich., Order No. 77-22088).

[42]W. B. Maier II, J. Chem. Phys. **61**, 3459 (1974).

[43]D. H. Katayama, T. A. Miller, and V. E. Bondybey, J. Chem. Phys. **72**, 5469 (1980).

[44]R. E. Fox, J. Chem. Phys. **35**, 1379 (1961).

[45]R. E. Winters, J. H. Collins, and W. L. Courchene, J. Chem. Phys. **45**, 1931 (1966).

[46]M. R. Flannery and T. F. Moran, J. Phys. B **9**, 509 (1976).

[47]As discussed by Märk (Ref. 48), the dissociative ionization cross section is increased by 5% to correct for N^+ ions with near thermal energies and decreased by 8.8% to be consistent with the total ionization measurements of Ref. 25.

[48]T. D. Märk, J. Chem. Phys. **63**, 3731 (1975).

[49]Märk's measurement (Ref. 48) was normalized to the single ionization cross section of Ar. Both the shape and magnitude of the Ar^+ curve given in Ref. 48 disagree with his more recently published data (Ref. 50). If the earlier N_2 data is corrected for what appears to be systematic errors, the curve agrees with that derived from Rapp and Englander–Golden in shape and is only about 14% lower in magnitude.

[50]K. Stephen, H. Helm, and T. D. Märk, J. Chem. Phys. **73**, 3763 (1980).

[51]Using our best estimates for the quantities in Eq. (3) $[I^+/\gamma F^0]$ $= (1.17 \pm 0.21) \times 10^{-8}$, $A^0 \cong 0.086 \pm 0.013$ cm^2, $v^0 = 8.3 \times 10^6$ cm/s, $w \cong 0.3$ cm, $F^- = F^-$(measured)K(geometrical correction factor) $= (2.75 \times 10^{14}/s)$ (0.38), $\gamma(N_2, 1 \text{ keV}) \cong \gamma(N_2^+, 1 \text{ keV}) = 0.5 \pm 0.2$, we deduce that the absolute ionization cross section of N_2 $(X \, ^1\Sigma_g^+)$ at 28.2 eV is $(1.3 \pm 0.6) \times 10^{-16}$ cm^2. Rapp and Englander–Golden (Ref. 25) give 0.995×10^{-16} cm^2 at 28 eV.

[52]N. G. Utterback and B. Van Zyl, Phys. Rev. Lett. **20**, 1021 (1968); N. G. Utterback and B. Van Zyl, J. Chem. Phys. **68**, 2742 (1978); *Abstracts of the Eleventh International Conference on the Physics of Electronic and Atomic Collisions*, (Society for Atomic Collision Research, Kyoto, Japan, 1979) (Aug.–Sept. 1979), p. 842; N. G. Utterback (private communication).

[53]K. H. Krebs, Fortschr. Phys. **16**, 419 (1968).

[54]E. Bauer and C. D. Bartkey, J. Chem. Phys. **43**, 2466 (1965).